

Peridynamic simulation of elastic wave propagation by applying the boundary conditions with the surface node method

Francesco Scabbia^{1,a,*}, Mirco Zaccariotto^{1,2}, Ugo Galvanetto^{1,2}, Florin Bobaru³

¹ Centro di Ateneo di Studi e Attività Spaziali “Giuseppe Colombo” (CISAS), Università degli Studi di Padova, Padova, 35131, Italy

² Industrial Engineering Department (DII), Università degli Studi di Padova, Padova, 35131, Italy

³ Department of Mechanical and Materials Engineering, University of Nebraska-Lincoln, Lincoln, NE, USA

^a francesco.scabbia@phd.unipd.it

Keywords: Peridynamics, Wave Propagation, Surface Node Method, Surface Effect, Nonlocal Boundary Conditions

Abstract. Peridynamics is a novel nonlocal theory able to deal with discontinuities, such as crack initiation and propagation. Near the boundaries, due to the incomplete nonlocal region, the peridynamic surface effect is present, and its reduction relies on using a very small horizon, which ends up being expensive computationally. Furthermore, the imposition of nonlocal boundary conditions in a local way is often required. The surface node method has been proposed to solve both the aforementioned issues, providing enhanced accuracy near the boundaries of the body. This method has been verified in the cases of quasi-static elastic problems and diffusion problems evolving over time, but it has never been applied to a elastodynamic problems. In this work, we show the capabilities of the surface node method to solve a peridynamic problem of elastic wave propagation in a homogeneous body. The numerical results converge to the corresponding peridynamic analytical solution under grid refinement and exhibit no unphysical fluctuations near the boundaries throughout the whole timespan of the simulation.

Motivation

When structures are exposed to unfavorable conditions, e.g., high temperature gradients, hostile environmental actions, excessive mechanical loading, or extreme events, cracks may initiate, propagate, and coalesce over time, compromising the functionality of the affected structure. Aircraft integrity assessments often consist of scheduled maintenance to inspect damage propagating in the structures. The first concern is the safety of passengers since in between two scheduled inspections, little can be said about the status of the aircraft so that an unexpected failure could bring catastrophic consequences. The second drawback is related to financial losses, as each airplane has to be grounded for several hours/days during inspections.

Fracture is difficult to predict because of complex multiphysical interactions and multiscale mechanisms that influence the behavior/evolution of cracks and damage. The capability of currently available computational tools based on classical mechanics, such as the Finite Element Method, to describe crack propagation and fragmentation is rather limited. On the other hand, the peridynamic theory allows to model fracture phenomena with ease.

Introduction to the peridynamic theory

Peridynamics (PD) is a nonlocal continuum theory based on integro-differential equations [1,2]. Peridynamics is more general compared to classical continuum models based on partial differential equations since discontinuities in the unknown displacements can arise and evolve in the domain without leading to mathematical inconsistencies or singularities in the problem. Successful

applications of this theory are, for instance, initiation and propagation of cracks in solid bodies [3,4], damage mechanisms in corrosion (with autonomously evolving interfaces) [5], etc.

In a PD body B , a point interacts with all the points within a finite distance δ , named *horizon size*. As shown in Fig. 1, the neighborhood H_x is the set of points with which a generic point x interacts:

$$H_x = \{x' \in B: |x' - x| \leq \delta\} . \tag{1}$$

Each interaction between any points x and x' is called *bond*. Thus, the PD equation of motion for a generic point x in a 1D, homogeneous, linear elastic body [6,7] is given as

$$\ddot{u}(x, t) = v^2 \int_{H_x} \frac{u(x', t) - u(x, t)}{\delta(x' - x)^2} dx', \tag{2}$$

where u is the displacement, \ddot{u} is the acceleration and v is the wave speed.

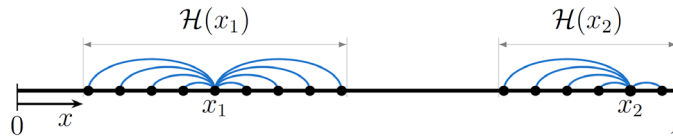


Figure 1: Example of the neighborhoods of two points (x_1 and x_2) in a peridynamic body. Note that the neighborhood of point x_2 is incomplete due to the closeness with the boundary of the body, whereas the neighborhood of point x_1 in the bulk of the body is complete. The blue curved lines represent the PD bonds between points x_1 , x_2 , and their neighboring points, respectively.

However, nonlocal theories are well-known to have issues near the boundaries of the body, for the reason illustrated in Fig. 1. Due to the lack of some bonds, points near the boundaries of the body exhibit an apparent variation in stiffness properties, if one uses the same micromodulus for bonds of points near the boundaries as for bonds of points in the bulk. This phenomenon is called *peridynamic surface effect* and is usually undesired in structural analyses [8-10]. Moreover, nonlocal models require the imposition of nonlocal boundary conditions, i.e., loads and constraints have to be enforced in a layer of finite thickness. This is in contrast with the concept of local boundary conditions that are enforced just at the boundary of the body. Since experiments generally provide measurements at the boundary, imposing local boundary conditions in a nonlocal model is usually desired. In this work, the surface node method (see details in the following) is used to mitigate the PD surface effect and impose local boundary conditions in the peridynamic model. This method has been applied to quasi-static mechanical problems [9-11] and to a diffusion problem evolving over time [12]. Here we extend it to elastodynamic problems in 1D. Further extensions to higher dimensions are immediate.

Discretization in space and time

A peridynamic body is commonly discretized by means of the meshfree method with a uniform grid spacing Δx [13]. Therefore, each node is representative of a cell of length Δx , as shown in Fig. 2. After the discretization in space, the peridynamic equation of motion of a generic node i is written as

$$\ddot{u}(x_i, t) = \frac{v^2}{\delta} \sum_{j \in H_i} \frac{u(x_j, t) - u(x_i, t)}{(x_j - x_i)^2} \beta_{ij} \Delta x , \tag{3}$$

where x_i and x_j are respectively the coordinates of node i and any node j within the neighborhood H_i of node i , and β_{ij} is the quadrature coefficient of node j with respect to H_i . β_{ij} is defined as the fraction of cell of node j which actually lies within the neighborhood H_i [14,15]. Hence, $\beta_{ij} = 1$ if the cell of node j lies completely inside H_i and $0 < \beta_{ij} < 1$ if the cell of node j lies partially inside H_i .

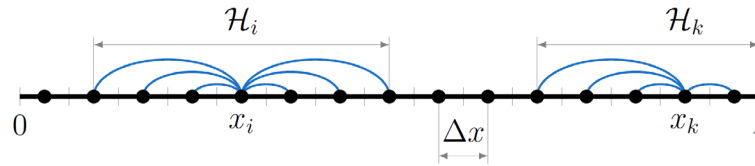


Figure 2: Discretization of the peridynamic body by means of the meshfree method with a uniform grid spacing Δx . The black solid dots and the blue curved lines represent the nodes and the bonds, respectively.

The explicit central difference is employed to integrate in time [13]:

$$\ddot{u}(x_i, t_n) = \frac{u(x_i, t_{n+1}) - 2u(x_i, t_n) + u(x_i, t_{n-1}))}{\Delta t^2}, \quad (4)$$

where Δt is the time step size and n stands for the index of the current time step. Therefore, the iterative procedure to obtain the displacement of node i at the time step $n + 1$ is determined by the following formula:

$$u(x_i, t_{n+1}) = 2u(x_i, t_n) - u(x_i, t_{n-1}) + \frac{(v\Delta t)^2}{\delta} \sum_{j \in H_i} \frac{u(x_j, t) - u(x_i, t)}{(x_j - x_i)^2} \beta_{ij} \Delta x. \quad (5)$$

The initial displacement $u(x_i, t_0)$ and velocity $\dot{u}(x_i, t_0)$ are known at any node. However, to obtain the displacement at the first time step $u(x_i, t_1)$, the knowledge of $u(x_i, t_{-1})$ is required as well. This displacement can be computed as

$$u(x_i, t_{-1}) = u(x_i, t_0) - \dot{u}(x_i, t_0)\Delta t + \ddot{u}(x_i, t_0) \frac{\Delta t^2}{2}, \quad (6)$$

where

$$\ddot{u}(x_i, t_0) = \frac{v^2}{\delta} \sum_{j \in H_i} \frac{u(x_j, t_0) - u(x_i, t_0)}{(x_j - x_i)^2} \beta_{ij} \Delta x. \quad (7)$$

Review of the Surface Node Method

Let us call *interior nodes* the nodes lying within the peridynamic body. In order to complete the neighborhoods of the interior nodes near the boundaries of the body, two fictitious domains are added at the two boundaries of the body, as shown in Fig. 3. The nodes lying in the fictitious domains are named *fictitious nodes*. Moreover, we introduce the *surface nodes* at the two ends of the body, a new type of nodes that do not have PD bond connections with other nodes and are used to impose the peridynamic boundary conditions in a local way.

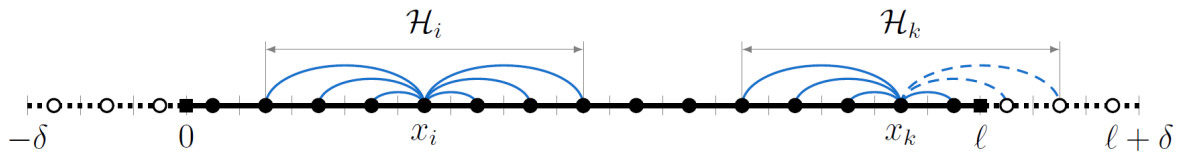


Figure 3: Introduction of the fictitious domain to complete the neighborhoods of the nodes near the boundaries of the body. The solid and empty dots represent the interior and the fictitious nodes, respectively. The solid squares at $x = 0$ and $x = l$ represent the surface nodes. The solid and dashed blue lines represent the bonds between nodes.

In this work, we apply only Dirichlet boundary conditions at the surface nodes, i.e., the displacements of the surface nodes are constrained. For the imposition of Neumann boundary conditions, the equations enforced at the surface nodes based on the peridynamic force flux can be found in [9-12]. To determine the displacements of the fictitious nodes, we assume that a fictitious domain deforms as the corresponding closest surface node. In other words, we determine the displacements of a fictitious node f via a Taylor-based extrapolation, truncated at the linear term for simplicity:

$$u(x_f, t_n) = u(x_s, t_n) + (x_f - x_s) \frac{\partial u(x_s, t_n)}{\partial x}, \tag{8}$$

where the derivative of the displacement at the surface node s is computed with the finite difference method as

$$\frac{\partial u(x_s, t_n)}{\partial x} = \frac{u(x_s, t_n) - u(x_p, t_n)}{x_s - x_p}, \tag{9}$$

where p is the index of the interior node closest to the surface node s . Note that, by plugging Eq. 9 into Eq. 8, the displacements of the fictitious nodes are functions of the displacements of the surface node and of its closest interior node. An example of the Taylor-based extrapolation is illustrated in Fig. 4. At this point, since the displacements of the surface nodes are prescribed as boundary conditions, the only unknowns are the displacements of the interior nodes, which can be found by solving, at each time step, the system of equations generated by Eq. 5.

Analytical solution of elastic wave propagation in Peridynamics

Even though Peridynamics handles with ease the treatment of discontinuities thanks to the integro-differential equations, determining analytical solutions to such equations is a much more difficult task to accomplish. For this reason, peridynamic numerical results are often compared with those obtained with classical mechanics. However, due to the different formulations of the theories, analytical solutions to the peridynamic and classical problems may be (and usually are) different from one another, and even more so in dynamics. A recent work [6,7] has shown that the method of separation of variables can be applied to peridynamic models to obtain their analytical solutions. Therefore, we present here one of the examples in [7] with the analytical solution to a peridynamic elastodynamic (elastic wave propagation) problem.

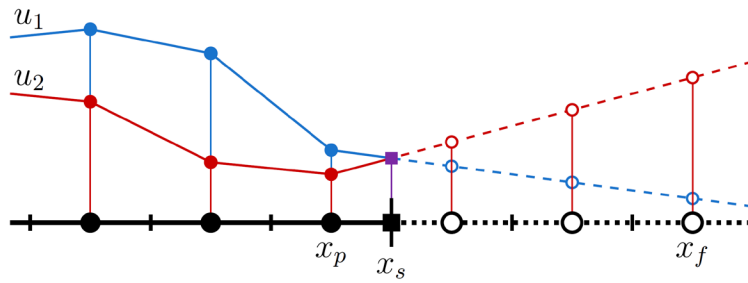


Figure 4: Examples of displacement field (u_1 and u_2 at two different time steps) determined by a linear Taylor-based extrapolation over the fictitious domain when Dirichlet boundary conditions are enforced at the surface node (purple square). The displacements of the fictitious nodes (empty dots) depend on the value of the constraint and the displacement of the interior node closest to the boundary.

The initial boundary value problem of wave propagation in a peridynamic medium is given as

$$\begin{cases} \ddot{u}(x, t) = \frac{v^2}{\delta} \int_{H_x} \frac{u(x', t) - u(x, t)}{(x' - x)^2} dx' & \text{for } 0 < x < \ell, \quad t > 0, \\ u(0, t) = u(\ell, t) = 0 & \text{for } t > 0, \\ u(x, 0) = 0.02e^{-100(x-0.5)^2}, \quad \dot{u}(x, 0) = 0 & \text{for } 0 < x < \ell, \end{cases} \quad (10)$$

where ℓ is the length of the peridynamic body. Note that the initial displacement field $u(x, 0)$ has the shape of a Gaussian function. The analytical solution to this peridynamic problem is computed by means of the method of separation of variables [6,7]:

$$u(x, t) = \sum_{m=1,3,5,\dots}^{\infty} \frac{0.004\sqrt{\pi}}{\ell} \sin\left(\frac{m\pi}{2}\right) e^{\frac{-k_m^2}{400}} \sin(k_m x) \cos(v\sqrt{-\psi} t), \quad (11)$$

where $k_m = \frac{m\pi}{\ell}$ and $\psi = \psi(\delta)$ is the nonlocal factor computed as

$$\psi(\delta) = \frac{2}{\delta^2} [k_m \delta \text{Si}(k_m \delta) + \cos(k_m \delta) - 1], \quad (12)$$

where $\text{Si}(\cdot)$ is the sine integral function. The analytical solution in Eq. 11 will be used as reference for the numerical results.

Results and discussion

In this section, we solve numerically the problem in Eq. 10 of the peridynamic wave propagation in a homogeneous, linear elastic body by using the meshfree discretization in space and the explicit central difference method for time integration (Eq. 5). This is the first application of the Surface Node Method to an elastodynamic problem.

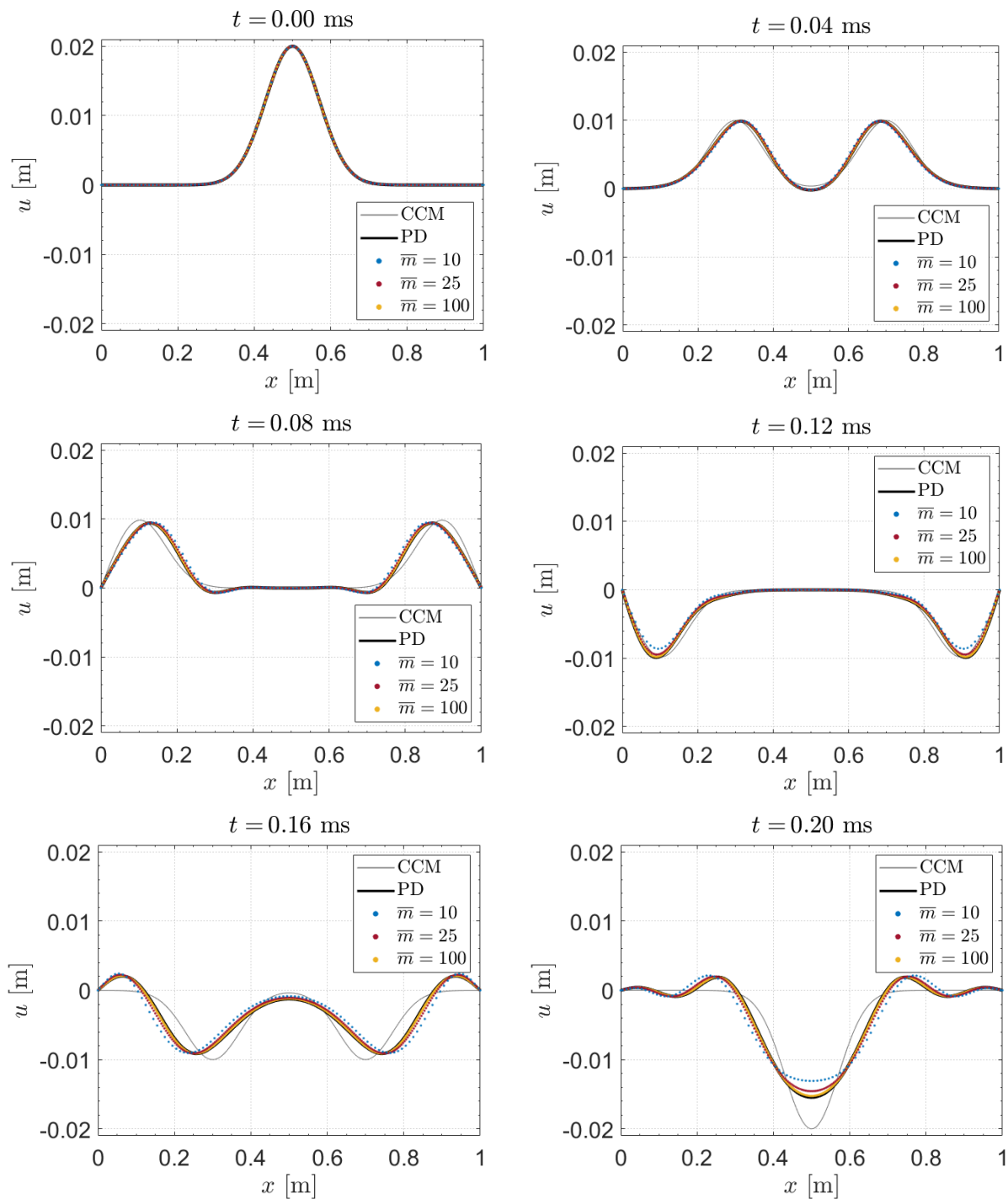


Figure 5: Plots of the propagating wave at different instants of time t . Note that the Classical Continuum Mechanics (CCM) analytical solution is a non-dispersive wave, whereas the peridynamic (PD) analytical solution with $\delta = 0.1\ell$ is a dispersive wave. The peridynamic numerical results (with $\delta = 0.1\ell$) are represented by the colored dots corresponding to the displacements computed at each node. As the grid is refined (namely as the \bar{m} -ratio $\bar{m} = \delta/\Delta x$ is increased keeping δ constant), the numerical results converge to the peridynamic analytical solution.

The length of the body is assumed to be $\ell = 1$ m and the horizon size $\delta = 0.1\ell$. The wave speed is computed as $v = \sqrt{E/\rho}$, where $E = 200$ GPa is the Young's modulus and $\rho = 8000$ kg/m³ is the density. Regarding the time integration, we used a time step size of $\Delta t = 0.0002$ ms to discretize a total timespan of $T = 0.2$ ms. The series to compute the analytical solution in Eq. 11 is truncated after the first 40 terms. In order to prove that the numerical model converges to the peridynamic analytical solution, different grid sizes are adopted. Since the horizon size has a fixed value, the grid refinement is equivalent to increasing the value of the \bar{m} -ratio, defined as $\bar{m} = \delta/\Delta x$, i.e., increasing the number of nodes lying within a neighborhood. This is why, in Peridynamics, the convergence analysis related to the grid refinement is called \bar{m} -convergence. Therefore, we choose $\bar{m} = 10, 25, 100$, corresponding to a grid spacing $\Delta x = 10, 4, 1$ mm and a number of interior nodes $N = 100, 250, 1000$, respectively.

Fig. 5 shows the analytical solutions obtained with Classical Continuum Mechanics (CCM) and Peridynamics (PD), and the peridynamic numerical results. We observe that in this simple dynamic problem the CCM solution cannot serve as reference solution for the numerical PD cases since it is clearly different from the exact PD solution. Moreover, note that elastic waves modeled with CCM are non-dispersive, but this is not the case for waves propagating in a peridynamic medium [1,7]. The dispersion in a peridynamic medium can be reduced by decreasing the horizon size δ , since the PD solution approaches the CCM one as $\delta \rightarrow 0$ [7,16].

The peridynamic numerical results are close to the PD analytical solution at any instant of time and their accuracy is improved by increasing the value of the \bar{m} -ratio, as expected in a \bar{m} -convergence analysis. No unphysical fluctuations or kinks, typically observed in relation to surface effect and/or nonlocal boundary conditions (see for example [8-11]), are exhibited near the boundaries of the body. Therefore, the Surface Node Method has been shown to be accurate and reliable in the solution of dynamic problems.

Conclusions

The peridynamic framework is a promising theory to model fracture phenomena in solid bodies. However, the intrinsic nonlocality of the model leads to the well-known peridynamic surface effect and fluctuations of the solution of an elastodynamic problem near the boundaries of the body. Moreover, there is the need for a method to impose local boundary conditions in these nonlocal models. The surface node method provides an easy and automatic way to considerably reduce the oscillations near the boundaries and impose local boundary conditions in a peridynamic model. In this work, we verified that the surface node method is accurate when applied to solve an elastodynamic problem in a homogeneous, linear elastic body. In particular, we showed that the numerical results exhibit no unphysical fluctuations near the boundaries and converge to the peridynamic analytical solution under grid refinement.

Acknowledgements

The authors would like to acknowledge the support they received from the Italian Ministry of University and Research under the PRIN 2017 research project "DEVISU" (2017ZX9X4K) and from University of Padova under the research project BIRD2020 NR.202824/20.

References

- [1] S.A. Silling, Reformulation of elasticity theory for discontinuities and long-range forces, *J. Mech. Phys. Solids* 48 (2000) 175-209. [https://doi.org/10.1016/S0022-5096\(99\)00029-0](https://doi.org/10.1016/S0022-5096(99)00029-0)
- [2] S.A. Silling, M. Epton, O. Weckner, J. Xu, E. Askari, Peridynamic states and constitutive modelling, *J. Elast.* 88 (2007) 151-184. <https://doi.org/10.1007/s10659-007-9125-1>
- [3] F. Bobaru, G. Zhang, Why do cracks branch? A peridynamic investigation of dynamic brittle fracture, *Int. J. Fract.* 196 (2015) 59-98. <https://doi.org/10.1007/s10704-015-0056-8>

- [4] M. Zaccariotto, F. Luongo, U. Galvanetto, G. Sarego, Examples of applications of the peridynamic theory to the solution of static equilibrium problems, *Aeronaut. J.* 119 (2015) 677-700. <https://doi.org/10.1017/S0001924000010770>
- [5] Z. Chen, F. Bobaru, Peridynamic modeling of pitting corrosion damage, *J. Mech. Phys. Solids* 78 (2015) 352-381. <https://doi.org/10.1016/j.jmps.2015.02.015>
- [6] Z. Chen, X. Peng, S. Jafarzadeh, F. Bobaru, Analytical solutions of peridynamic equations. Part I: transient heat diffusion, *J. Peridyn. Nonlocal Model* (2022) 303-335. <https://doi.org/10.1007/s42102-022-00080-7>
- [7] Z. Chen, X. Peng, S. Jafarzadeh, F. Bobaru, Analytical solutions of peridynamic equations. Part II: elastic wave propagation, *submitted*.
- [8] Q.V. Le, F. Bobaru, Surface corrections for peridynamic models in elasticity and fracture, *Comput. Mech.* 61 (2018) 499-518. <https://doi.org/10.1007/s00466-017-1469-1>
- [9] F. Scabbia, M. Zaccariotto, U. Galvanetto, A novel and effective way to impose boundary conditions and to mitigate the surface effect in state-based Peridynamics, *Int. J. Numer. Methods. Eng.* 122 (2021) 5773-5811. <https://doi.org/10.1002/nme.6773>
- [10] F. Scabbia, M. Zaccariotto, U. Galvanetto, A new method based on Taylor expansion and nearest-node strategy to impose Dirichlet and Neumann boundary conditions in ordinary state-based Peridynamics, *Comp. Mech.* 70 (2022) 1-27. <https://doi.org/10.1007/s00466-022-02153-2>
- [11] F. Scabbia, M. Zaccariotto, U. Galvanetto, A new surface node method to accurately model the mechanical behavior of the boundary in 3D state-based Peridynamics, *J. Peridyn. Nonlocal Model* (2023) 1-35. <https://doi.org/10.1007/s42102-022-00094-1>
- [12] F. Scabbia, M. Zaccariotto, U. Galvanetto, F. Bobaru, Stability and convergence analyses for peridynamic models with autonomously evolving interfaces, *in preparation*.
- [13] S.A. Silling, E. Askari, A meshfree method based on the peridynamic model of solid mechanics, *Comput. Struct.* 83 (2005) 1526-1535. <https://doi.org/10.1016/j.compstruc.2004.11.026>
- [14] P. Seleson, Improved one-point quadrature algorithms for two-dimensional peridynamic models based on analytical calculations, *Comput. Methods Appl. Mech. Eng.* 282 (2014) 184-217. <https://doi.org/10.1016/j.cma.2014.06.016>
- [15] F. Scabbia, M. Zaccariotto, U. Galvanetto, Accurate computation of partial volumes in 3D peridynamics, *Eng. Comput.* (2022) 1-33. <https://doi.org/10.1007/s00366-022-01725-3>
- [16] S.A. Silling, R.B. Lehoucq, Convergence of peridynamics to classical elasticity theory, *J. Elast.* 93 (2008) 13-37. <https://doi.org/10.1007/s10659-008-9163-3>